X-ray Structure and AM1 Studies of the Proton-Transfer Adduct between 2,5-Dihydroxy-p-quinone and 4-(N,N-Dimethylamino)pyridine

ARTICLE *in* THE JOURNAL OF PHYSICAL CHEMISTRY · MAY 1996

Impact Factor: 2.78 · DOI: 10.1021/jp953211c

X-ray Structure and AM1 Studies of the Proton-Transfer Adduct between 2,5-Dihydroxy-*p*-quinone and 4-(*N*,*N*-Dimethylamino)pyridine

Mario Bossa, Marcello Colapietro, Giorgio O. Morpurgo,* Simone Morpurgo, and Gustavo Portalone

Dipartimento di Chimica, Università degli Studi di Roma "La Sapienza", P.le A. Moro 5, 00185 Roma, Italy

Received: October 30, 1995; In Final Form: February 26, 1996[⊗]

The structure of the crystalline 1:1 adduct obtained by reacting 2,5-dihydroxy-*p*-quinone (DH*p*Q) and 4-(*N*,*N*-dimethylamino)pyridine (DAPY) has been determined by X-ray single-crystal diffraction. The compound consists of ribbons of the two components linked by proton-transfer bonds. Each bond is due to a proton of the 4-(*N*,*N*-dimethylamino)pyridinium cation (r(N−H) = 1.13 Å), bifurcated between two oxygen atoms of the monoprotonated anion. Antiparallel stacks of DH*p*Q−DAPY adducts are present in the solid. According to AM1 and molecular mechanics calculations, it has been shown that the interaction between stacked adducts is the prerequisite for the establishing of proton-transfer bonds ($O^-\cdots HN^+$) between DH*p*Q and DAPY. It is suggested that electrostatic interactions such as the dipole−dipole coupling play a major role in establishing this type of hydrogen bond within each stack.

Introduction

Model studies of amine oxidase, an enzyme from bovine serum (BSAO, E.C. 1.4.3.6), suggested that, in the resting state, the coenzyme 2,4,5-trihydroxy phenylalanine quinone (TPQ) forms a proton-transfer complex with some basic group of the protein ($O^-\cdots HB^+$) or with water.[1] The adducts formed by 2,5-dihydroxy-*p*-quinone (DH*p*Q) with N-bases, such as substituted pyridine or imidazole, were chosen as models. In nondissociating solvents (e.g., CH_2Cl_2) the 1:1 adducts were found to exist in two equilibrium forms: a yellow hydrogen-bonded species (R−OH···N-base) and a proton-transfer compound ($R-O^-\cdots HN^+$-base), absorbing at 480 nm. The latter form becomes predominant with bases of large pK_a value. In absence of structural data, the problem of hydrogen bond formation was addressed by the AM1 molecular orbital method[2] (on 1:1 DH*p*Q−N-base models).[3,4] The system energy was optimized at imposed proton positions along the reaction coordinate from DH*p*Q to N-base, and a double-minimum potential energy curve was obtained. The deepest minimum at r(O−H) = 1.0 Å corresponds to a hydrogen-bonded OH···N adduct; the other minimum at r(O−H) ≈ 1.9 Å corresponds to the proton-transfer complex ($O^-\cdots HN^+$). The energy separation between the two minima (0.6−1.0 eV, depending on the base considered) suggests the formation of the hydrogen-bonded compound (OH···N), in contrast with experimental data. These calculations were performed on the isolated system. Inclusion of solvent effects or packing effects in the solid state is expected to produce more realistic results.

The solid substances, which can be precipitated from concentrated alcoholic solutions of the proton donor and different proton acceptors, are either yellow or red. Red crystals suitable for X-ray structure determinations were recently prepared for the 1:1 adduct of DH*p*Q and 4-(*N*,*N*-dimethylamino)pyridine (DAPY), allowing to check the validity of previously forwarded hypotheses.

The present paper reports the X-ray structure of the compound and shows that the AM1 optimized structure[1] is in agreement with the experimental one. The paper also shows that the interaction between adduct units is an essential factor in promoting proton transfer within the crystal, as suggested by recent investigations on the crystal structure of self-assembling hydrogen-bonded aggregates.[5]

Experimental Section

Materials. The 1:1 adduct of DH*p*Q and DAPY (pK_a = 9.7) was synthesized by mixing equimolar concentrated solutions of the components in methanol. Red microcrystals separated.[1] The crude product was recrystallized from absolute ethanol. Suitable crystals for X-ray structure determination were obtained by first producing sizable crystals by the very slow cooling of a hot saturated solution of the compound in methanol. The size was then increased by dipping the crystals into a saturated methanolic solution, which was allowed slow evaporation, alternate with additions of small amounts of solvent, in order to dissolve tiny crystals possibly formed. The size could also be increased by subjecting the saturated methanolic solution containing the crystals to repeated heating (40 °C, 8 h) and cooling (20 °C, 16 h) over the course of several weeks.

Microcrystals of a yellow, hydrogen-bonded 1:2 adduct of DH*p*Q with 4-cyanopyridine (pK_a = 1.8) were precipitated from saturated methanolic solutions of the components. The solid adduct is unstable and, on standing, slowly tinges orange because of DH*p*Q separation. Solutions aging or heating also cause the dissociation of the compound into its separate components.

X-ray Structure. Crystal and experimental data are summarized in Tables 1 and 2. A suitable crystal, of approximately 0.2 × 0.2 × 0.3 mm, was mounted on a CS automatic four-circle diffractometer equipped with a Huber goniometer using graphite monochromatized Mo Kα radiation (λ = 0.710 69 Å). The cell parameters were refined by least squares from the angular position of nine high-order reflections. A total of 2396 reflections were collected using a $\omega-2\theta$ scan technique at room temperature with 3.0° ≤ 2θ ≤ 60° in the octants h, k, ±l; R_{int} = 0.0237. The scan rate was automatically chosen according to the peak intensity in the range 2.0−30.0° min^{-1}. The background was measured for a half of the scanning time at each end of the scan. The intensities of three standard reflections, monitored every 97 reflections during the data collections, showed no appreciable decay. Data were corrected for Lorentz and polarization effects, but not for absorption. A total of 1272 independent reflections having $|F_o| \geq 4\sigma|F_o|$ were used in all subsequent calculations.

The structure was solved by direct methods.[6] The difference electron density map showed all H atoms, and the hydrogen at

* To whom correspondence should be addressed.

[⊗] Abstract published in *Advance ACS Abstracts,* May 1, 1996.

S0022-3654(95)03211-4 CCC: $12.00

TABLE 1: Crystal Data for 2,5-Dihydroxy-*p*-quinone−4-(*N*,*N*-dimethylamino)pyridine Adduct

$C_{13}H_{14}N_2O_4$, fw = 262.265, monoclinic	
$a = 12.731(11)$, $b = 7.031(3)$, $c = 13.605(4)$ Å	
$\beta = 90.63(6)°$, $V = 1217.7(12)$ Å^3	
$\rho_{cal} = 1.431$ g cm^{-3}	
$Z = 8$, $P2_1/a$, $\mu = 1.159$ cm^{-1}, $F(000) = 552.0$	
no. of measured reflections	2396
no. of unique reflections	1476
no. of observed reflections, $\|F_o\| \geq 4\sigma\|F_o\|$, n	1272
function minimized	$\sum w(\|F_o\| - \|F_c\|)^2$
variables refined, m	216
a, b, and c values in the weighting function[a]	1.6229, 0.1616, 0.0009
R[b]	0.0724
R_w[c]	0.1014
goodness of fit, S[d]	1.083

[a] $w = 1.0/(a + b|F_o| + c|F_o|^2)$. [b] $R = \sum(|F_o|^2 - F_c|^2)/\sum|F_o|^2$. [c] $R_w = \sum w(|F_o|^2 - |F_c|^2)/\sum w|F_o|^2$. [d] $S = \sum w(|F_o| - |F_c|)^2/(n - m)$.

TABLE 2: Final Coordinates and Equivalent Values of the Anisotropic Temperature Factors for Non-H Atoms with ESD's in Parentheses

atom	*x*	*y*	*z*	B_{eq}[a]
O7	0.6055(3)	0.6703(7)	0.0691(3)	4.4(1)
O8	0.7901(3)	0.5958(6)	0.1570(3)	4.0(1)
O9	0.6093(3)	0.5466(7)	0.4556(3)	4.4(1)
O11	0.4294(3)	0.6134(7)	0.3663(3)	4.2(1)
C1	0.5157(4)	0.6135(8)	0.3103(4)	2.9(1)
C2	0.5111(4)	0.6493(9)	0.2135(4)	3.5(2)
C3	0.6059(4)	0.6435(8)	0.1570(4)	2.9(1)
C4	0.7107(4)	0.6010(8)	0.2103(4)	3.0(1)
C5	0.7091(4)	0.5732(9)	0.3120(4)	3.5(2)
C6	0.6169(4)	0.5724(8)	0.3647(4)	2.0(1)
N15	0.6964(4)	0.1291(7)	0.0415(3)	3.8(1)
C16	0.5932(5)	0.1510(9)	0.0646(4)	3.7(2)
C17	0.5590(4)	0.1429(8)	0.1576(4)	3.5(2)
C18	0.6299(4)	0.1115(8)	0.2367(4)	2.9(1)
C19	0.7364(4)	0.0887(9)	0.2102(4)	3.5(2)
C20	0.7661(5)	0.0993(9)	0.1161(4)	3.9(2)
N23	0.5991(3)	0.1023(7)	0.3300(3)	3.7(1)
C26	0.4890(6)	0.1127(10)	0.3545(6)	4.0(2)
C27	0.6746(6)	0.0759(10)	0.4115(5)	4.6(2)

[a] $B_{eq} = {}^4/_3\sum_i\sum_j b_{ij}(\mathbf{a}_i\mathbf{a}_j)$.

the ring N atom of DAPY was clearly located. The final refinement was carried out by full-matrix least-squares techniques, with the H atoms treated isotropically and the other atoms anisotropically. Each hydrogen atom linked to carbon was arbitrarily assigned the equivalent isotropic temperature factor of the parent atom. The final difference Fourier map, with a root-mean-square deviation of electron density of 0.1 e Å^{-3}, showed values not exceeding 0.4 e Å^{-3} which, however, are not of chemical significance. Atomic scattering factors were taken from ref 7. Fractional atomic parameters for non-H atoms are listed in Table 2. All calculations[8] were done on a PC using the SIR CAOS[9] and CRYSTALS[10] programs.

Theoretical Methods. *Ab initio* calculations[11] and semiempirical molecular orbital calculation methods such as AM1 and PM3[12,13] could be used, in principle, for the present research. However, the more accurate *ab initio* methods were considered inconvenient for the study of large molecular systems with the size comparable with that treated here, because of the computational time which would have been required. On the other hand, geometries obtained from the above semiempirical methods show a general agreement with the structures obtained from X-ray crystallographic data.[14,15] AM1 and PM3 were also recognized to give reliable results for calculations related to hydrogen bonding.[16] The calculations of the present work have been performed with AM1 to facilitate the comparison of the results with those previously reported on related systems.[1,3,4]

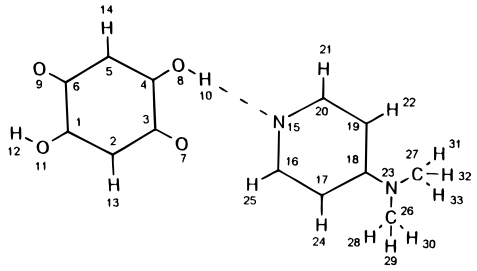

Figure 1. Atom numbering system adopted for the DH*p*Q−DAPY and DH*p*Q$^-$−DAPYH adducts.

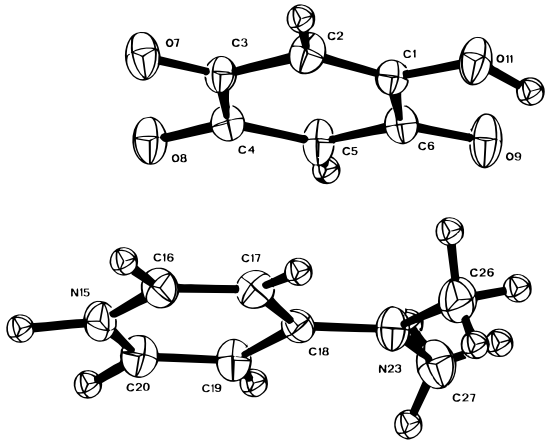

Figure 2. Drawing of the 1:1 molecular adduct of DH*p*Q$^-$ and DAPYH showing the anisotropy of the thermal motion. The thermal ellipsoids are scaled to the 30% probability level. The drawing is based on the atomic parameters from the final refinement.

Geometry Optimization. Energy levels were calculated and minimized by means of the semiempirical AM1 method supplied by the code HyperChem Release 4 (1994, Hypercube, Inc.) on the molecular systems DH*p*Q−DAPY (Figure 1), DH*p*Q−MPY, and DH*p*Q−PY (where MPY = 4-(methylamino)pyridine and PY = pyridine), each of them in monomeric and stacked polymeric form. First-derivative analysis and Polak−Ribiere[17] algorithm were employed for geometry optimization. The convergence criteria adopted were an energy gradient of 0.02 kcal mol^{-1} Å^{-1} for the isolated monomeric adducts and of 0.1 kcal mol^{-1} Å^{-1} for the stacked polymeric forms. The optimized structures of monomeric species were found coincident with those previously calculated and minimized by means of the AM1 method provided by MOPAC (version 4.10).[4]

HyperChem molecular mechanics force field MM+,[17] an extension of MM2,[18] was also used because of its usefulness in treating systems formed by a large number of atoms as the octamers (see text). The atomic charges previously derived from AM1 analysis were employed in the MM+ calculations. No distance cutoffs were imposed to electrostatic interactions. For the DAPY molecule a geometrical constraint had to be introduced in order to keep the plane of the $-N(CH_3)_2$ group parallel to the plane of the pyridine ring. Geometry optimization algorithm and convergence criteria were the same as those employed at the semiempirical level.

Results

Crystallographic Investigation. The atom numbering scheme and the molecular structure of the 1:1 adduct between DH*p*Q and DAPY are shown in Figures 1 and 2. Selected atomic distances and bond angles are given in Table 3.

Molecular Geometry of DHpQ. DH*p*Q has been studied by X-ray diffraction as free acid[19] and dipotassium salt (DH*p*Q2K).[20] In the free acid the molecule, which lies in the crystal on a center of symmetry, is basically of quinonoid character, but some

TABLE 3: Intertomic Distances and Angles of the 2,5-Dihydroxy-*p*-quinone−4-(*N*,*N*-dimethylamino)pyridine Adduct Obtained from X-ray Structure (with ESD's in Parentheses), from AM1 and MM+ Calculations, Performed on Both the H-Bond and the Proton-Transfer Forms, as Isolated Monomer and as the Central Unit of a Stacked Trimer

		R−OH···N			R−O$^-$···HN$^+$		
	X-ray	AM1 monomer	AM1 trimer[a]	MM+ monomer	AM1 monomer	AM1 trimer[a]	MM+ monomer
C3−O7	1.211(6)	1.238	1.237	1.361	1.249	1.242	1.366
C4−O8	1.252(6)	1.360	1.358	1.359	1.270	1.256	1.398
C6−O9	1.256(6)	1.238	1.241	1.361	1.252	1.263	1.361
C1−O11	1.344(6)	1.365	1.367	1.359	1.362	1.370	1.359
C1−C2	1.340(8)	1.353	1.352	1.397	1.355	1.351	1.399
C2−C3	1.439(7)	1.458	1.460	1.395	1.452	1.460	1.396
C3−C4	1.541(7)	1.499	1.500	1.402	1.524	1.524	1.407
C4−C5	1.397(7)	1.356	1.357	1.397	1.393	1.410	1.393
C5−C6	1.382(7)	1.454	1.451	1.394	1.412	1.397	1.394
C6−C1	1.507(7)	1.499	1.497	1.402	1.509	1.504	1.405
O11−H12	0.95(6)	0.976	0.975	0.944	0.978	0.977	0.944
C18−N23	1.334(7)	1.399	1.398	1.360	1.370	1.361	1.361
C26−N23	1.446(9)	1.439	1.440	1.465	1.439	1.439	1.468
C27−N23	1.471(8)	1.439	1.440	1.465	1.438	1.444	1.468
C17−C18	1.414(8)	1.419	1.420	1.400	1.431	1.437	1.401
C18−C19	1.416(7)	1.419	1.420	1.400	1.430	1.436	1.401
C16−C17	1.343(8)	1.400	1.400	1.398	1.388	1.382	1.398
C19−C20	1.341(8)	1.400	1.400	1.397	1.389	1.383	1.398
C16−N15	1.363(8)	1.347	1.348	1.262	1.360	1.367	1.260
C20−N15	1.357(8)	1.347	1.347	1.262	1.361	1.364	1.260
N15−H10	1.13(7)	2.518	2.488	2.145	1.044	1.017	1.025
N15−O7	2.965(6)	3.632	3.578	3.607	2.833	2.920	2.831
N15−O8	2.717(6)	3.405	3.384	3.043	2.733	2.866	2.684
O7−H10	2.23(6)	2.270	2.274	2.485	1.984	2.070	2.031
O8−H10	1.65(6)	0.978	0.978	0.945	1.897	2.036	1.882
O7−C3−C2	122.0(5)	123.7	123.8	119.0	121.6	121.5	118.1
O7−C3−C4	119.4(4)	119.9	119.9	119.9	120.1	120.5	121.8
O8−C4−C3	115.6(4)	118.6	118.7	122.0	116.7	117.2	122.1
O8−C4−C5	126.2(5)	118.9	118.8	119.9	125.0	124.7	117.1
O9−C6−C1	115.9(4)	119.3	119.2	119.8	116.5	116.1	119.6
O9−C6−C5	125.9(5)	124.5	124.4	119.1	127.2	127.3	118.6
O11−C1−C2	122.0(5)	119.2	119.4	120.1	119.5	119.5	119.9
O11−C1−C6	114.9(4)	118.0	117.8	121.8	117.5	117.2	121.0
C1−C2−C3	119.5(5)	121.0	120.9	120.9	120.2	120.2	119.8
C2−C3−C4	118.7(4)	116.3	116.3	121.0	118.3	118.0	120.1
C3−C4−C5	118.2(4)	122.5	122.4	118.1	118.4	118.1	120.7
C4−C5−C6	122.3(5)	121.2	121.2	120.8	123.8	123.8	118.5
C5−C6−C1	118.1(5)	116.2	116.4	121.1	116.3	116.6	121.8
C6−C1−C2	123.1(5)	122.7	122.8	120.9	123.0	123.3	119.1
C26−N23−C27	117.4(5)	117.1	116.7	121.0	119.4	119.2	120.6
C26−N23−C18	120.8(5)	118.0	117.8	119.5	120.3	120.5	119.7
C27−N23−C18	121.8(5)	118.0	118.0	119.5	120.3	120.1	119.7
C17−C18−N23	122.6(5)	121.6	121.8	122.9	121.6	121.7	122.6
C19−C18−N23	121.9(5)	121.6	121.5	122.9	121.7	122.0	122.5
C17−C18−C19	115.5(5)	116.7	116.6	114.2	116.7	116.3	114.9
C16−C17−C18	120.8(5)	119.1	119.2	119.4	120.0	120.2	119.7
C18−C19−C20	121.1(5)	119.1	119.1	119.3	120.1	120.2	119.7
C17−C16−N15	122.5(5)	124.2	124.1	123.8	121.6	121.7	121.0
C19−C20−N15	122.3(5)	124.2	124.2	123.9	121.5	121.8	121.0
C16−N15−C20	117.9(5)	116.6	116.7	119.3	120.1	119.8	123.7

[a] The central adduct of the trimer is considered.

degree of conjugation has been observed to exist along the 1-oxopropen-3-ol chain. On the contrary DH*p*Q2K, which also lies in the crystal on a center of symmetry, shows a marked conjugation through the 1-oxopropen-3-olate chain.

In the adduct, DH*p*Q can be regarded as the intermediate between the free acid and the dipotassium salt. As shown in Table 3, there is an appreciable conjugation in the O8−C4−C5−C6−O9 chain, favored by the planarity of the molecule and the lack of a hydrogen atom due to protonation of the ring N of DAPY. The effect of conjugation is not observed for the remaining half part of the molecule. For instance, the observed C4−O8 (1.252(6) Å) and C6−O9 (1.256(6) Å) bond distances are significantly longer than the C3−O7 (1.211(6) Å) and shorter than the C1−O11 (1.344(6) Å) bond distances. Further the alternation of bond order shown by the carbon-carbon bond lengths in the O7−C3−C2−C1−O11 chain disappears when passing to the O8−C4−C5−C6−O9 chain.

Molecular Geometry of DAPY. DAPY has been determined in the crystal as free base[21] and as hydrochloride dihydrate (DAPYHCl).[22] Theoretical calculations on the electronic structure of aminopyridines[23] show that the protonation is easier at the ring N atom than at the amino N atom. By comparing the molecular geometry of DAPY in the 1:1 molecular adduct with DH*p*Q with those obtained for free DAPY and DAPYHCl, the protonation on the N ring is confirmed. For instance, it is well-known[24] that the valence angle of the pyridine N atom bearing a hydrogen atom is significantly larger than that of the N atom without any attachment. In the protonated DAPY of the adduct (DAPYH hereafter) the ring angle C16−N15−C20, 117.9(5)°, agrees with that found for the hydrochloride dihydrate derivative, 119.7 (2)°, and is larger by 3.4° than the corresponding angle in the free base, 114.5(2)°.

The atoms of the pyridine ring, which shows C_{2v} symmetry, are coplanar within the estimated standard deviations (0.006−0.007 Å), and the angle between the ring plane and the plane determined by atoms N23, C26, and C27 is 176.5°. This geometric conformation favors conjugation between the lone pair of the amino N atom and the π system of the ring.

The amino ring C18−N23 bond length, 1.334(7) Å, is nearly equal to the corresponding bond length in DAPYHCl, 1.339(3) Å, but shorter than in free DAPY, 1.367(2) Å. The value of the ring angle at C18 in DAPYH is 115.5(5)°, 2.9° smaller than

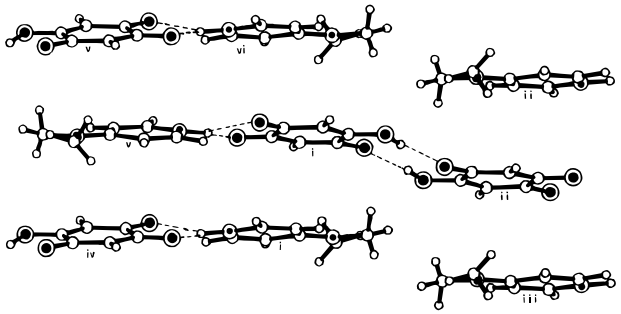

Figure 3. View of the crystal structure along the *b* axis. The symmetry operations relating the various molecules are (i) *x*, *y*, *z*; (ii) $1 - x$, $1 - y$, $1 - z$; (iii) $1 - x$, *y*, $1 - z$; (iv) $1.5 - x$, $-0.5 + y$, $-z$; (v) $1.5 - x$, $0.5 + y$, $-z$; (vi) *x*, $1 + y$, *z*. Oxygen and nitrogen atoms of the molecular adduct are marked by filled circles. The hydrogen bonds are indicated by the dashed lines.

that obtained for the corresponding angle in pyridine, 118.4(1)°,[25] 4.5° smaller than in 4-cyanopyridine,[26] 0.9° smaller than in 4-aminopyridine,[27] and in agreement with those found in free DAPY, 116.1(2)°, and in DAPYHCl, 116.0(2)°. The sensitivity of the ring angle at the place of substitution to the nature of the substituent has been established for a large number of benzenoid rings.[28] In analogy with what has been determined in monosubstituted benzene derivatives, the conjugation between the lone pair of the amino N atom and the π system of the ring accounts for the decreasing of the *ipso* angle observed in passing from pyridine to DAPY.

The shortness of C18−N23 bond and the decrease of the *ipso* angle are accompanied by variations in the bond lengths of the ring when compared with the corresponding bonds in pyridine. These variations can be summarized as follows: (*i*) a slight lengthening of the C18−C17 and C18−C19 bond lengths; their average value is 1.415(7) Å, which is 0.023 Å longer than in pyridine, 1.392(1) Å; (*ii*) a shortening of C16−C17 and C19−C20 bond lengths; their average value is 1.342(8) Å, which is 0.052 shorter than in pyridine, 1.394(1) Å; (*iii*) a slight lengthening of the C16−N15 and C20−N15 bond lengths; their average value is 1.360(8) Å, which is 0.022 Å longer than in pyridine, 1.338(1) Å.

The configuration assumed by the amino group and the changes observed in the molecular geometry of DAPYH are both consistent with some degree of conjugation between the substituent and the ring, suggesting a trend toward a quinonoidal structure.

Molecular Packing. A packing diagram of the crystal structure is shown in Figure 3. An extended network of hydrogen bonding is present. DH*p*Q is connected on one side through a centrosymmetric hydrogen bond 2.721(6) Å long to a symmetry-related DH*p*Q molecule and on the other side to a DAPYH molecule with two O···N hydrogen bonds 2.717(6) and 2.965(6) Å long. Infinite ribbons of molecules run nearly perpendicular to the *b* axis of the cell. Stacks where DH*p*Q molecules alternate DAPYH molecules are separated by approximately *b*/2.

The nature of stacking interactions between simple organic molecules was carried out by the analysis of the crystal structure.[29] For example, in the complex between *N*,*N*-dimethylaniline and fluoranil,[30] a system closely related for comparison to the present molecular adduct, the distance between the N atom of the amino group and the C atom of the carbonyl group is 3.03 Å, while the amino group has a more tetrahedral character than in the hexafluorobenzene complex with the same amine. It was concluded that in that complex there is a strong $n \rightarrow \pi^*$ charge-transfer interaction. In the present 1:1 molecular adduct the shortest intermolecular contact between neighboring molecules in the stacks, 3.346(8) Å, involves the N atom of the amino group of DAPYH and the C6 carbonyl of DH*p*Q monoanion. This result together with the finding that N amino atom lies on the pyridine ring plane and that the interplanar distance is higher than in the previous case, though shorter on the lone-pair side of the N amino atom than on the other side by 0.416(8) Å, makes a charge-transfer interaction questionable.

Theoretical Studies. AM1 calculations performed on the 1:1 DH*p*Q−DAPY adduct gave a curve for total energy vs O8−H10 distance characterized by a double minimum.[4] The deepest minimum, at 1.0 Å, corresponds to the adduct containing an OH···N bond, while the other minimum at 1.88 Å is 0.65 eV higher and represents the energy of the proton-transfer complex ($O^-\cdots HN^+$). Geometrical parameters obtained by applying the AM1 method on the monomeric adducts are reported in Table 3. It can be seen by comparison that the geometry predicted for the proton-transfer adduct is more closely related to that determined by the X-ray diffraction method than the hydrogen-bonded one. The adduct can be described as an essentially planar system formed by two molecules bound through a bifurcated hydrogen bond, where the base is in the pyridinium form. The conjugation in the O8−C4−C5−C6−C9 chain, determined from X-ray data and reflected in the shortening of the C4−O8 bond and the equalization of the C4−C5 and C5−C6 bond lenghts versus the values calculated for free DH*p*Q (1.36, 1.35, and 1.46 Å, respectively), is very well reproduced. The sequence of localized single and double bonds, typical of a quinonoid system, in the O7−C3−C2−C1−O11 chain also agrees with the experimental data. The DAPYH structure is close to that determined by X-ray. The quinonoid character of the molecule is evident in the shortening of the C18−N23, C16−C17, and C19−C20 bonds, with respect to those of the free DAPY (1.39, 1.40, and 1.40 Å, respectively). The calculated C17−C18−C19 angle, which is 116.7° in DAPYH (116.7° in DAPY, 115.9° in the free protonated form), is also comparable to the experimental value. However, the AM1 optimized geometry shows that H10 is at bonding distance from N15 (1.02 Å), with N15 almost equidistant from O7 and O8 (2.92 and 2.87 Å). The X-ray structure gives H10−N15 1.16 Å, thus appearing less definitely ionic, and locates N15···O7 and N15···O8 at 2.96 and 2.71 Å, respectively. Accurate calculations revealed the presence of a secondary minimum close to and connected with the deepest one along the reaction coordinate from oxygen to the pyridine nitrogen. The DH*p*Q proton would fall into this secondary minimum when forming an internal hydrogen bond with O7 in the absence of base (cf. O9···H12−O11 of Figure 1). By restraining the O8−H10 distance to 1.6 Å, which is the value determined by X-ray diffraction, the calculated structure of the proton-transfer adduct essentially agreed with that found in the solid.

The rather conspicuous energy difference between the heights of the two minima in the plot of total energy vs O8−H10 distance[3,4] was suggested to have arisen from the comparison of data concerning an isolated molecule with those derived from a crystalline structure. Attempts to releave this inherent reductionism of the molecule proceeded along two directions. AM1 calculations were performed on (i) the system obtained by adding a DH*p*Q molecule on the DH*p*Q side of the adduct, in order to better mimic a portion of the crystal layer, but this was seen not to produce any appreciable change of the proton-transfer potential curve, and (ii) the system formed by adducts stacked in an antiparallel mode to mimic crystal packing. The calculations were also extended to the adducts with pyridine and 4-methylpyridine. The stacks were formed by dimers, trimers, and, in the case of PY, also tetramers of adducts, each in both of the two stable conformations, namely, the hydrogen-

TABLE 4: Total Energy (E_{TOT}), Total Energy per Monomeric Unit (E_{MON}), and Dipole Moment Obtained by AM1 Calculations Performed on the Adducts of DH*p*Q and Respectively Pyridine, 4-Methylpyridine, and 4-(*N*,*N*-Dimethylamino)pyridine, as Isolated Monomer and as Stacked Polymers, in Both the Hydrogen-Bonded and the Proton-Transfer Form

system	E_{TOT} (eV mol^{-1})	E_{MON} (eV mol^{-1})	dipole (D)
DH*p*Q−PY	−3019.406	−3019.406	2.338
(DH*p*Q−PY)$_2$	−6038.817	−3019.408	0.034
(DH*p*Q−PY)$_3$	−9058.218	−3019.406	2.291
DH*p*Q$^-$−PYH	−3018.501	−3018.501	16.320
(DH*p*Q$^-$−PYH)$_2$	−6037.595	−3018.798	0.065
(DH*p*Q$^-$−PYH)$_3$	−9056.461	−3018.820	15.411
(DH*p*Q$^-$−PYH)$_4$	−12075.34	−3018.836	0.731
DH*p*Q−MPY	−3175.294	−3175.294	2.725
(DH*p*Q−MPY)$_2$	−6350.601	−3175.301	0.065
(DH*p*Q−MPY)$_3$	−9525.914	−3175.305	2.534
DH*p*Q$^-$−MPYH	−3174.434	−3174.434	17.195
(DH*p*Q$^-$−MPYH)$_2$	−6349.591	−3174.796	0.004
(DH*p*Q$^-$−MPYH)$_3$	−9524.413	−3174.804	15.495
DH*p*Q−DAPY	−3551.161	−3551.161	4.147
(DH*p*Q−DAPY)$_2$	−7102.317	−3551.116	1.767
(DH*p*Q−DAPY)$_3$	−10653.46	−3551.152	3.008
DH*p*Q$^-$−DAPYH	−3550.504	−3550.504	20.599
(DH*p*Q$^-$−DAPYH)$_2$	−7101.790	−3550.895	0.099
(DH*p*Q$^-$−DAPYH)$_3$	−10652.69	−3550.896	17.768

bonded and the proton-transfer one. The initial structural parameters required to start the geometry optimization were set equal to those previously calculated for the monomeric adducts. The interplanar distances were initially set at ca. 3 Å in all cases, and geometry optimization was first coarsely accomplished by molecular mechanics calculation (gradient ≃ 0.5 kcal mol^{-1} Å^{-1}) and then refined by AM1. After geometry optimization the adduct remained stacked in all cases.

The hydrogen-bonded adducts forming the stacks were planar as in the monomeric form and the distance between each plane was relevant, approaching 4.5 Å. Almost no gain in energy resulted from the stacking process so that its value, per monomeric unit, remained very close to that of the isolated adduct. The only sign of interaction is the coupling of the small dipole moment of the monomers (Table 4). The instability to heating and aging of the yellow hydrogen-bonded 1:2 crystalline compound of DH*p*Q and 4-cyanopyridine (cf. Experimental Section) might be due to the above lack of interaction.

The packing effect became, instead, relevant for proton-transfer adducts. Some deviation from planarity was observed, especially in the dimeric stacks of those formed with MPY and DAPY. When the base is PY, the two components in each layer are slightly disrotated along the major axis of the adduct because of the unequal interaction among the planes, due to the inherent asymmetry of DH*p*Q. With MPY and DAPY the deviation from planarity is larger, mainly because of the tendency of the methyl groups to hydrogen bond to the carbonyl of DH*p*Q which faces them, thus imparting to the dimers the profile of a convex lens. In all cases, however, the central adduct of trimeric stacked models remains planar. This is due to the compensating effect of having two adducts symmetrically facing the central one. Figure 4 illustrates some of the above results by comparing the optimized geometries of trimeric stacks of the proton-transfer adducts with PY and DAPY, respectively. The geometrical parameters of the central DAPY adduct of a trimeric stack (Table 3) are rather close to those of the isolated one. The O−H distance at the minimum of the proton-transfer curve remains ≃2.0 Å.

From Table 4 it is evident that the average energy value calculated per monomeric proton-transfer adduct of PY, MPY, and DAPY decreases with the increase of the stacked components. The increased number of interactions leads to a progressive stabilization of the proton-transfer adducts vs the hydrogen-bonded ones (Figure 5). The main energy factor responsible for the stabilization is the coupling of the large dipole moments (17−20 D) characteristic of the proton-transfer species. The calculated interplanar distance in the case of the central dimer of the tetramer of the PY adducts in the proton-transfer configuration is, as expected, lower than that corresponding to the hydrogen-bonded case (4.15 vs 4.50 Å). However, in this and the other examples examined, such a distance is different by excess to that experimentally determined on the DH*p*Q−DAPY crystals.

Further calculations were carried on by the molecular mechanics MM+ force field method. The systems examined were the stacked (DH*p*Q$^-$−DAPYH)$_n$ and (DH*p*Q−DAPY)$_n$

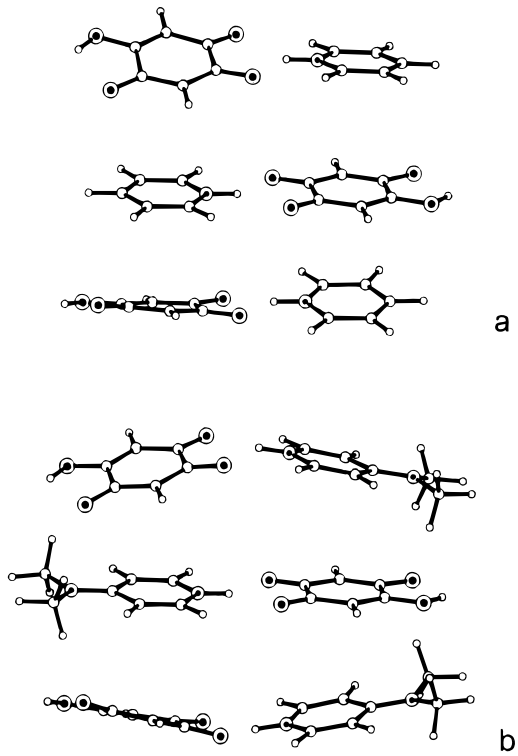

Figure 4. Optimized geometries of trimeric proton-transfer stacks: DH*p*Q$^-$−PYH (a) and DH*p*Q$^-$−DAPYH (b).

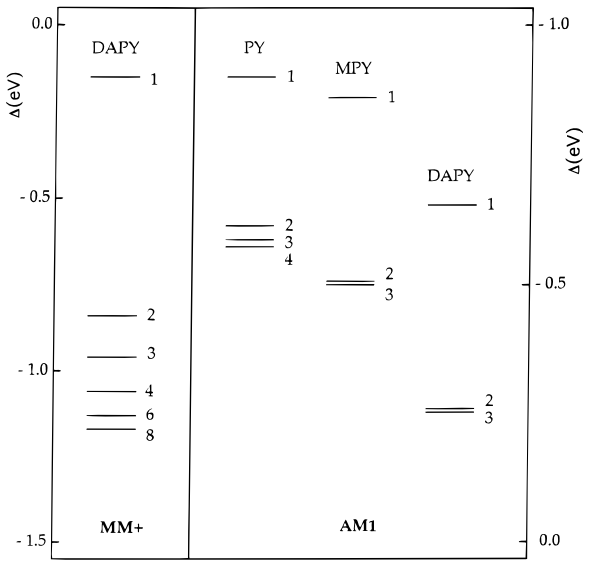

Figure 5. Variation of the difference in total energy (eV) per monomeric unit between the hydrogen-bonded (OH···N) and the proton-transfer (O$^-$···HN$^+$) form of the DH*p*Q−N-base adducts vs the multiplicity of monomers (*n*) in each stack. MM+ data (left) and AM1 data (right).

TABLE 5: Electronic Energy (E_{EL}), Total Energy (E_{TOT}), and Total Energy per Monomeric Unit (E_{MON}) Obtained from MM+ Calculations Performed on the DH*p*Q$^-$−DAPYH Adducts in Stacked Polymeric Form and on the DH*p*Q−DAPY Adduct in Monomeric Form

system	E_{EL} (eV mol^{-1})	E_{TOT} (eV mol^{-1})	E_{MON} (eV mol^{-1})
DH*p*Q$^-$−DAPYH	−0.883	−0.275	−0.275
(DH*p*Q$^-$−DAPYH)$_2$	−2.541	−1.934	−0.967
(DH*p*Q$^-$−DAPYH)$_3$	−3.833	−3.261	−1.087
(DH*p*Q$^-$−DAPYH)$_4$	−5.287	−4.751	−1.188
(DH*p*Q$^-$−DAPYH)$_6$	−8.013	−7.576	−1.263
(DH*p*Q$^-$−DAPYH)$_8$	−10.787	−10.393	−1.299
DH*p*Q−DAPY	−0.426	−0.129	−0.129

adducts (n = 1, 2, 3, 4, 6, 8). The overall geometry of the monomeric (n = 1) adducts was found in reasonable agreement with that calculated by AM1 (Table 3), though the finest details were not expected to be reproduced by force field methods.

Geometry optimization up to a gradient of 0.1 kcal mol^{-1} Å^{-1} resulted in a disarray of the initially stacked hydrogen-bonded adducts ($n \geq 2$), accompanied by the breaking of the O−H···N bonds. When the calculations were repeated to optimize the proton-transfer systems, each adduct remained intact and parallel to the others with an interplanar distance of ca. 3.5 Å. The energy per monomer in these cases was always smaller than that calculated for a hydrogen-bonded adduct, becoming more negative with the increase of n (Table 5 and Figure 5).

Conclusions

The X-ray structure determination confirms the previous suggestion made on the presence of a proton-transfer bond O$^-$···HN$^+$ between DH*p*Q and DAPY in the crystals obtained by mixing these two components in alcohol. The AM1 semiempirical quantum-mechanical method reasonably accounts for the structure of the adduct. The trend observed in X-ray determined bond lengths and angles, on going from separate DH*p*Q monoanion and protonated DAPY (data nonintegrally reported in the present paper) to the proton-transfer adduct, is also reproduced by calculation. The interaction of monomeric adducts in the stacking process justifies the formation of proton-transfer compounds, as the latter become stabilized with respect to the hydrogen-bonded adduct, in contrast with what is found in vacuo. The energetic is only approximate, especially for those stacks formed with few monomeric adducts in the form of proton-transfer compounds, as they somewhat deviate from planarity. This effect, which fades by increasing the number of components in a stack, is to be ascribed to the tendency of the methyl groups of N(CH$_3$)$_2$ of DAPY to hydrogen-bond the carbonyl of the next adduct. This effect is not to be considered as an artifact due to AM1, as it occurs also by employing PM3, a calculation method which is known not to overestimate nonbonded atom interactions. In addition, methyl−carbonyl interactions have recently been detected experimentally.[31] Stacking is theoretically not allowed to hydrogen-bonded adducts, which, according to the calculations, tend to form a collection of independent molecules. This fact probably explains the instability of the crystalline products of DH*p*Q with low-pK_a N-bases.

The nature of the stacking interaction is a debated matter.[32] In the present case a main contribution is very likely provided by the electrostatic interaction due to antiparallel coupling of the monomers, as revealed by the strong reduction of dipole moment on going from monomeric to polymeric form of DH*p*Q−N-base compounds. This hypothesis has some support by the success of molecular mechanics calculations which are known to only treat molecular systems in terms of analytical functions. Table 5 shows that classical electrostatic interactions supply the most relevant contribution to the total energy of the systems. It is worth noting that the agreement occurring between the calculated and the experimentally determined interplanar distance is very good. AM1, instead, is likely to overestimate the π-electron repulsion of the face-to-face stacked orientation, thus giving a higher interplanar distance.

Supporting Information Available: Tables of anisotropic displacements, structure factors, and H atom coordinates (8 pages). Ordering information is given on any current masthead page.

References and Notes

(1) Bossa, M.; Morpurgo, G. O.; Morpurgo, L. *Biochemistry* **1994**, *33*, 4425.
(2) Dewar, M. J. S.; Zoebisch, E. G.; Healy, E. F.; Stewart, J. J. P. *J. Am. Chem. Soc.* **1985**, *107*, 3902.
(3) Bossa, M.; Morpurgo, G. O.; Morpurgo, L. *J. Mol. Struct. (THEOCHEM)* **1993**, *287*, 269.
(4) Bossa, M.; Morpurgo, G. O.; Morpurgo, L. *J. Mol. Struct. (THEOCHEM)* **1995**, *330*, 395.
(5) Rectz, M. T.; Hoger, S.; Harms K. *Angew. Chem. Int. Ed Engl.*. **1994**, *33*, 181 and references therein.
(6) Burla, M. C.; Camalli, M.; Cascarano, G.; Giacovazzo, C.; Polidori, G.; Spagna, R.; Viterbo, D. *J. Appl. Crystallogr.* **1989**, *22*, 389.
(7) *International Tables for X-Ray Crystallography*; Kynoch Press: Birmingham, 1974; Vol. IV, p 99.
(8) Further details of the crystal structure determination, including values for anisotropic displacements, structure factors, and H atom coordinates, have been deposited as Supporting Information.
(9) Camalli, M.; Capitani, D.; Cascarano, G.; Giacovazzo, C.; Spagna, R. Italian Patent No. 35403c/86, *SIR CAOS User Guide*, Istituto di Strutturistica Chimica CNR: Rome, Italy.
(10) Watkin, D. J.; Carruthers, P. W.; Betteridge, P. W. *CRYSTALS User Guide*; Chemical Crystallography Laboratory: Oxford, England, 1985.
(11) Hehre, W. J.; Radom, L.; Schleyer, P. v. R.; Pople, J. A. *Ab Initio Molecular Thory*; Wiley: New York, 1986.
(12) Stewart, J. J. P. *J. Comput. Chem.* **1989**, *10*, 209.
(13) Stewart, J. J. P. *J. Comput. Chem.* **1989**, *10*, 221.
(14) Belletete, M.; Leclerc, M.; Durocher, G. *J. Phys. Chem.* **1994**, *98*, 9450.
(15) Shelver, W. L.; Rosenberg, H.; Shelver, W. H. *J. Mol. Struct. (THEOCHEM)* **1994**, *312*, 1.
(16) Vinson, L. K.; Dannenberg, J. J. *J. Am. Chem. Soc.* **1989**, *111*, 2777.
(17) *HyperChem Computational Chemistry*; Hypercube, Inc. Waterloo, Ontario, Canada, 1994; Chapter 10, p 154.
(18) Allinger, N. L. *J. Am. Chem. Soc.* **1977**, *99*, 8127.
(19) Semmingsen, D. *Acta Chem. Scand.* **1977**, *B31*, 11.
(20) Kulpe, S. *J. Prakt. Chem.* **1974**, *316*, 353.
(21) Ohms, U.; Guth, H. *Z. Kristallogr.* **1984**, *166*, 213.
(22) Chao, M.; Schempp, E.; Rosenstein, R. D. *Acta Crystallogr.* **1977**, *B33*, 1820.
(23) Konishi, H.; Kato, H.; Yonezewa, T. *Theor. Chim. Acta* **1970**, *19*, 71.
(24) Singh, C. *Acta Crystallogr.* **1965**, *19*, 861.
(25) Sørensen, G. O.; Mahler, L.; Rastrup-Andersen, N. *J. Mol. Struct.* **1974**, *20*, 119.
(26) Liang, M.; Sparrow, N.; Sommerville, P. *Acta Crystallogr.* **1971**, *B27*, 1986.
(27) Chao, M.; Schempp, E. *Acta Crystallogr.* **1977**, *B33*, 1557.
(28) *Accurate Molecular Structures: Their Determination and Importance*; Domenicano, A., Hargittai, I., Eds.; International Union of Crystallography and Oxford University Press: Oxford, 1992.
(29) Dahl, T. *Acta Chem. Scand.* **1994**, *48*, 95.
(30) Dahl, T. *Acta Chem. Scand.* **1981**, *A35*, 701.
(31) Desiraju, G. R.; Kashini, S.; Coombs, M. M.; Glusker, J. P. *Acta Crystallogr.*, **1993**, *B49*, 880.
(32) Hunter, C. A. *Chem. Soc. Rev.* **1994**, 101 and references therein.

JP953211C